Atmospheric Environment 319 (2024) 120312

Contents lists available at ScienceDirect

Atmospheric Environment

journal homepage: www.elsevier.com/locate/atmosenv

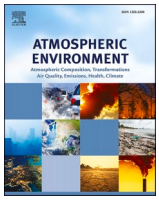

Another one bites the dust – Two street canyons studied with magnetic biomonitoring and OSPM modelling

Jukka Limo [a,*], Mari Kauhaniemi [b], Petriina Paturi [c], Jukka-Pekka Keskinen [b], Ari Karppinen [b], Joni Mäkinen [a]

[a] University of Turku, Department of Geography and Geology, FI-20014, Turku, Finland
[b] Finnish Meteorological Institute (FMI), 00101, Helsinki, Finland
[c] University of Turku, Department of Physics and Astronomy, FI-20014, Turku, Finland

HIGHLIGHTS

- Magnetic biomonitoring effective in evaluating air quality modelling.
- Street canyons prone to high magnetic PM concentrations.
- PM concentrations show discrepancies between OSPM model and magnetic biomonitoring.
- Street canyon characters and winter conditions caused inhomogeneous emissions.

ARTICLE INFO

Keywords:
Air quality
Environmental magnetism
Particulate matter
Urban pollution
Moss bag

ABSTRACT

Urban areas form a mosaic of microenvironments and structures, such as street canyons that are susceptible to elevated levels of traffic related pollutants. Street canyons are a relevant topic in air quality research and modelling since they are prone to reduced natural ventilation and when exposed to increased traffic emissions, can pose a serious risk to public health. We applied magnetic biomonitoring using moss bags to evaluate the quality of Operational Street Pollution Model (OSPM) and to study vertical distribution of modelled particulate matter (PM), magnetic PM and heavy metal pollution in a street canyon in Turku and Helsinki, Finland. Moss bags were attached on opposite sides of the streets at 3-, 6-, 9- and 12-m heights for 44 days in late autumn. Samples were analysed for mass-specific magnetic susceptibility (χ), hysteresis parameters and elemental components. High χ values and elemental concentrations of Fe, Al, Ti, Zn, Mn, Cu and Ba were found in both street canyons. Compared to measurements with airborne magnetic PM, the OSPM model underestimated the difference in PM concentrations between the opposite street canyon faces and overestimated the dilution of PM concentrations with altitude. In Turku the results between the OSPM model and magnetic measurements were incompatible. We suspect this is due to meteorological model input data from a distant weather station, street canyon features and a high slope angle contributing to non-uniform emissions in the street canyon. We demonstrate that the moss bag technique is a versatile tool to understand the small-scale variations of concentrations in a variety of complex urban environments.

1. Introduction

Road traffic in urban areas is a major source of airborne particulate matter (PM) and heavy metals. In addition to exhaust particles, the non-exhaust particles are generally released to the urban atmosphere by corrosion of vehicles and mechanical wear of their components (e.g. tyres, brakes, engines, clutches) as well as erosion of road surfaces (Kupiainen, 2007; Ozaki et al., 2004; Thorpe and Harrison, 2008; Ward, 1990). Urban magnetic PM is typically composed of iron oxides and magnetite (Fe3O4) is commonly the dominant magnetic mineral within the urban particulate composition (Matzka and Maher, 1999; Muxworthy et al., 2022; Salo et al., 2012; Sheikh et al., 2022). Magnetic PM occurs in various size fractions within the urban PM depending on whether combustion, friction or road erosion is the source. The

* Corresponding author. Department of Geography and Geology, University of Turku, FI-20014, Turku, Finland.
E-mail address: jukka.limo@utu.fi (J. Limo).

https://doi.org/10.1016/j.atmosenv.2023.120312
Received 4 August 2023; Received in revised form 20 November 2023; Accepted 15 December 2023
Available online 19 December 2023

dispersion of such pollutants is highly affected by suspension and resuspension of material because of traffic induced turbulence (Zhu et al., 2002; Zhang and Wexler, 2004). Nevertheless, the distribution of anthropogenic pollution is a result of the overall mass of the released pollution, the effective height of the emission, the surface roughness, atmospheric stability and wind conditions (Mathias et al., 2006). Since most of the global population inhabit urban areas, PM poses a serious global health threat and its treacherous capability to incorporate noxious heavy metals (e.g. Cd, Co, Cr, Cu, Mn Ni, Pb, Sb and Zn) (Sezgin et al., 2003; Yang et al., 2010) makes it especially harmful. According to EEA (2013a), solely in the EU, 88 % of the people living in urban areas are exposed to PM concentrations that exceed the outdated pre-2022 reference values determined by WHO and related respiratory and cardiovascular diseases are increasing (Özkan et al., 2016).

Modern urban areas are comprised of a diversity of microenvironments; therefore, it is particularly complicated to extensively monitor urban air quality with satisfactory spatiotemporal resolution, let alone to accurately model such a versatile milieu without a rather high level of uncertainty. The urban structures include open and closed spaces, low and high-rise buildings, motorways and pedestrian zones, tunnels and bridges and various-sized park areas. Potential pollution hotspots can arise in association with high population and traffic densities. Moreover, poor air dispersion conditions result in situations where exposure to harmful substances is significantly increased (Kumar et al., 2011; Vardoulakis et al., 2003). High pollution levels have been detected in urban street canyons, where a relatively narrow street is confined by buildings on both sides (Pirjola et al., 2012; Weber et al., 2006). Within these specific street environments, pedestrians, cyclists, motorists and residents may be exposed to levels of harmful substances that exceed the recommended regulatory limit values (Kumar et al., 2008; Vardoulakis et al., 2003). As street canyons are prone to reduced natural ventilation, subsequently leading to increase in concentrations, they pose a serious risk to public health and have therefore, become of great interest for air quality research and modelling.

The vertical dispersion of pollution within a particular street canyon is driven by factors such as geometry and aspect ratio (e.g. height/width – H/W and length/height – L/H ratio) (Vardoulakis et al., 2003), street orientation (Hoydysh and Dabbert, 1998) and synoptic wind conditions (Britter and Hanna, 2003) that all influence the direction of flow and the level of turbulence inside the canyon. The mixing within the canyon results from the ventilation flux of air from the canyon (Caton et al., 2003), wind induced turbulence (De Paul and Sheih, 1985), traffic (Solazzo et al., 2007) and atmospheric instability (Xie et al., 2005). The rooftop wind speed mainly dictates the shape and strength of wind vortices in the street canyon. However, local winds are further affected by urban roughness elements (e.g. balconies, slanted roofs, trees) (Guyev and Savory, 1999), turbulent mixing caused by passing vehicles (Eskridge and Rao, 1986), atmospheric stability and thermal effects caused by a varying degree of heating of the canyon walls and/or bottom (Kim and Baik, 2001; Sini et al., 1996). Nevertheless, a single vortex cell inside the canyon will be maintained by wind speeds in the range of 2–5 m s^{-1} moving perpendicular to a canyon with a H/W ratio of 1.5, but when ambient wind speeds drop below 1.5 m s^{-1} the vortex dissipates (De Paul and Sheih, 1986). Field and wind tunnel measurements have demonstrated increasing concentrations of pollutants from traffic on the leeward side of street canyons (De Paul and Sheih, 1985; Park et al., 2004) and decreasing particulate concentrations in association with an increasing altitude from ground to rooftop level (Kumar et al., 2009a; Pakkanen et al., 2003; Väkevä et al., 1999).

Numerous models are used to predict or represent the dispersion of pollutant concentrations within street canyons. However, relatively simple mathematical models have been utilized to support field measurements in order to attain and interpret time series of pollutant concentrations, such as the commonly used semi-empirical parametric Operational Street Pollution Model (OSPM) (Berkowicz, 2000). Vardoulakis et al. (2007) and Kumar et al. (2009b) compared measured concentrations of CO, NO_X, PM_{10} and particle number concentrations (PNCs) with representations of two different, but widely used dispersion models. Their findings suggest that OSPM produces annual means reasonably well, but it has shortcomings in estimating short-term or episodical concentrations, although the vertical profile of dilution is presented reasonably well, especially as it considers the turbulence generated by wind and traffic. Wang and Xie (2009) have also shown that the OSPM has a good estimation accuracy of primary pollutant averages at street level and on the opposite sides of the canyon. In estimating the concentrations of PM_{10}, the OSPM shows good agreement with field measurements (Assael et al., 2008; Hu and Zhong, 2010). To account for non-exhaust particle emissions, a more refined model has been generated that is adjusted to evaluate the suspension of PM_{10} emissions (Kauhaniemi et al., 2011). However, the evaluation of street canyon models is hindered by the lack of experimental data and applicability of the available data.

High spatiotemporal resolution of instrumental PM monitoring in street canyons is extremely difficult and usually requires expensive measurement configurations. Recently, a method known as magnetic biomonitoring has been used very successfully in urban areas to monitor PM and related elements (Limo et al., 2018; Salo et al., 2012; Salo and Mäkinen, 2019). Magnetic biomonitoring can be applied to various biological organisms e.g. lichens, *Tillandsia* spp. And leaves (Castañeda-Miranda et al., 2020; Gómez et al., 2021; Posada et al., 2023) or alternatively measured in situ (Chaparro et al., 2020; Marié et al., 2018). Active biomonitoring applied with moss bags allows a good spatial resolution for data collection with long sampling periods and a cost-effective option for extensive monitoring of urban air quality. Mosses do not have a root system or a cuticle, which means that they absorb all the necessary nutrients by dry and wet deposition from the air. Their high cation exchange capacity increases the absorbance capability to entrap air pollutants from the ambient air (Brown and Bates, 1990). As shown by Tretiach et al. (2011), moss bags are efficient in entrapping particle sizes of $PM_{2,5}$ and PM_{10} and the genus *Sphagnum* has frequently been used in several studies of urban pollution (Ares et al., 2015; Di Palma et al., 2019; Shvetsova et al., 2019; Zinicovscaia et al., 2018). However, only a few studies have emphasized vertical dispersion of pollution within street canyons (De Nicola et al., 2013; Goryainova et al., 2016; Vuković et al., 2013, 2015), and only one study has focused on using biomonitoring with moss bags for evaluating a street canyon model (Lazić et al., 2016). Accordingly, the use of magnetic biomonitoring to evaluate a street canyon dispersion model is an empty niche with potential for more research to focus on non-exhaust particles.

The aim of this study was to evaluate the results of an operational street pollution model by using magnetic biomonitoring with moss bag sampling. The main objectives were to investigate the vertical dispersion of urban airborne magnetic PM pollution within two separate street canyons by using magnetic biomonitoring and to compare the results with the dispersion of PM pollutants predicted by the OSPM model within the same period. Firstly, we hypothesise that our measurements are a good proxy for the vertical profile of PM concentrations in both the leeward and windward sides of the canyon. Secondly, we want to assess if the OSPM model will be able to produce results that represent the dispersion of PM pollution in accordance with the field measurements. We endeavour to increase the understanding of the pollutant dispersion and dilution processes in urban environments and thereby promote alternative approaches for future city planning to reduce pollution hotspots.

2. Materials and methods

2.1. Study area

The studied street canyons located in Helsinki in southern Finland (60°10′41′′N, 24°55′39′′E) and Turku in southwestern Finland (60°27′16′′N, 22°16′18′′E). Helsinki is the largest city and capital of

Finland, having an area of 719 km^2 with ca. 645 000 citizens. Turku is the fifth largest city with an area of 306.4 km^2 and ca. 180 000 citizens. The street canyons of Runeberginkatu (R) in Helsinki and Aninkaistenkatu (A) in Turku (Fig. 1) were used for sampling.

Runeberginkatu is 24 m wide and runs in north-south direction (6°–186°). It is 23 m high on both sides of the street, forming a symmetric, regular (H/W = 0.96) and long (L/H = 7.61) street canyon. The building structure on the western side of the street canyon is uniform across 175 m, whereas the eastern side has a small junction at ca. 38.5 m north of the measurement site. A two-way tramline runs in the middle of the street.

Aninkaistenkatu is 23 m wide, northwest-southeast oriented (326°–146°) and 23 m high on both sides of the street. It could be described as symmetric, regular (H/W = 1.00) and medium length (L/H = 5.22) street canyon. The street canyon section lies on a hill and it has a 6.9 % slope gradient. The western side has a uniform building structure across 120 m but the eastern side has a small junction ca. 38 m north of the measurement site.

2.2. Sampling design

The preparation of the moss bags follows the Finnish standard SFS 5794 (Finnish Standards Association, 1994). The moss *Sphagnum papillosum* was collected from a remote bog in Finland. Litter and unwanted organic material were manually removed in the laboratory. The moss was washed in 0,5 M HCl and rinsed with deionized H2O to balance the element levels. Using a cotton thread, circa 15 g of moist moss was enclosed in a polyamide net (0.64 cm^2 mesh). Part of the pre-processed moss was used as a control sample and analysed for the averages of initial magnetic and element concentration (CS 1 and 2). Three control sites from the surroundings of both city areas were used to obtain the rural background levels of pollutants (Table 1). To illustrate the precise pollutant accumulation during the study period, the background magnetic and elemental values were deducted from the moss bag data (Table 2).

Each vertical sampling site included three moss bags (subsamples) hanging from a wooden rod. The rods were attached to rainwater pipes on the opposite sides on the canyon walls at the heights of 3, 6, 9 and 12 m. At both street canyon locations, two reference samples were placed on the northern and southern ends of the street sections to reflect the general concentrations of pollutants released by the onsite traffic. The field study was conducted in late autumn after the annual leaf abscission of deciduous trees and before the snow season. The sampling continued

Table 1
Summary of background sample sites in Helsinki (BGH) and Turku (BGT).

	Location	Distance from site (km)	Direction
Helsinki			
BGH 1	Suomenlinna Sea Fortress	5	SE
BGH 2	Nuuksio	32	NW
BGH 3	Hynnä	31	N
Turku			
BGT 1	Erikvalla	14	SE
BGT 2	Laulainen	25	NW
BGT 3	Mäkkylä	16	NE

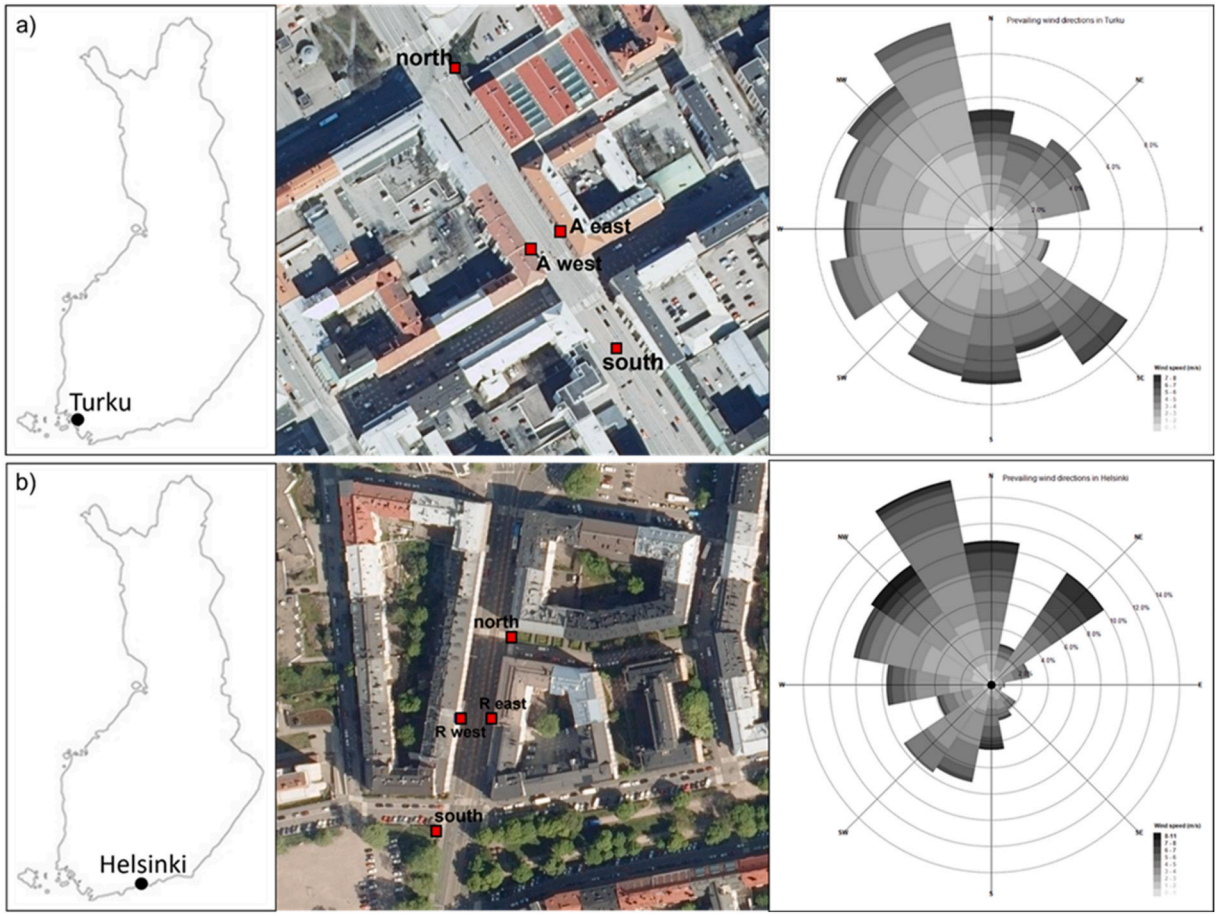

Fig. 1. Sampling locations of the street canyons a) Turku Aninkaistenkatu (60°27′16′′N, 22°16′18′′E) b) Helsinki Runeberginkatu (60°10′41′′N, 24°55′39′′E). The wind rose diagrams indicate prevailing wind direction and strengths during the sampling period (FMI weather stations Artukainen, Turku and Kaisaniemi, Helsinki). National Land Survey of Finland, https://asiointi.maanmittauslaitos.fi/karttapaikka/.

Table 2
Minimum detection limits (MDL) for analysed elements and initial average mass-specific magnetic susceptibilities (χ x $10^{-8}m^3kg^{-1}$) and element concentrations of control samples (CS) and background samples for Turku (BGT) and Helsinki (BGH).

	χ	Al	Ba	Cd	Co	Cr	Cu	Fe	Mn	Mo	Ni	Sb	Sr	Ti	V	W	Zn
MDL		1	0.1	0.01	0.01	0.1	0.01	1	1	0.01	0.1	0.02	0.5	1	2	0.1	0.1
CS1	−0.15	50	1.1	0.005	0.08	2.5	1.02	140	2	0.14	0.2	0.1	0.25	4	1	0.05	2.4
CS2	−0.20	50	1.2	0.005	0.19	2.3	1.09	150	1	0.12	0.2	0.09	0.25	4	1	0.05	2.6
BGT 1	−0.15	50	2.2	0.01	0.27	2.3	1.38	170	12	0.14	0.3	0.13	0.6	6	1	0.05	27.0
BGT 2	−0.15	50	1.8	0.005	0.25	2.3	1.17	150	1	0.14	0.3	0.11	0.25	5	1	0.05	7.4
BGT 3	−0.15	50	1.8	0.005	0.14	2.3	1.15	160	2	0.14	0.2	0.11	0.25	5	1	0.05	10.8
BGH 1	1.30	100	2.8	0.03	0.41	2.6	2.42	250	4	0.16	0.4	0.19	1.7	7	1	0.2	29.6
BGH 2	−0.20	50	1.4	0.01	0.22	2.3	1.28	160	2	0.12	0.3	0.11	0.5	4	1	0.05	6.0
BGH 3	−0.25	50	1.8	0.01	0.14	3.2	1.08	150	6	0.12	0.2	0.09	0.5	4	1	0.05	17.3

for 44 days from November 5 to December 18, 2016. During the biomonitoring period at Aninkaistenkatu and Runeberginkatu, the average daily air temperatures were −0.69 and −1.20 °C, the prevailing wind directions SE-NNW and SW-N, the average daily wind speeds 2.75 and 3.98 m s^{-1} and total rainfall 67.20 and 84.60 mm, respectively. The collected three subsamples were intermixed and air-dried at a constant 35 °C. The dried samples were ground with a Retsch PM100 planetary ball mill using a zirconium oxide (ZrO^2) grinding jar and balls. The samples were stored in 10 cm^3 air proof plastic containers.

2.3. Magnetic measurements

Mass-specific magnetic susceptibility (χ x 10^{-8} m^3 kg^{-1}) indicates the concentration of magnetic minerals in a sample. It was measured using a low frequency setting with a Bartington MS2B dual-frequency (0,465 and 4650 kHz) susceptibility meter in the Department of Geography and Geology, University of Turku. Each sample, canyon site (n = 20), background site (n = 6) and control sample (n = 2), were separated to two subsamples and weighed in standard 10 cm^3 measuring capsule. The holder cup correction of −0.2 was acquired by measuring five empty sample cups. Each subsample was measured five times with air measurements before and after the sample measurement. This gives a total average of ten measurements per sample. For samples AE12, A south and BGH 1 the sample material was not enough to fill two separate measuring capsules. In this case, the samples were re-intermixed after the first measurement, and weighed and measured again.

The magnetic mineral composition and grain-size distributions were examined by using magnetic hysteresis loop measurements with Quantum Design MPMS SQUID XL magnetometer in the department of Physics and Astronomy, University of Turku. A constant temperature of 300 K in a magnetic field between positive 1 T and negative 1 T was used to measure hysteresis properties. Saturation magnetisation (M_S), saturation remanence (M_{RS}), coercive force (H_C), and coercivity of remanence (H_{CR}) were acquired when first subtracting the linear diamagnetic signal from the 1 ml sample cup and sample holder and K of the cleaned moss using a fitting function:

$$M(B) = M_S \times ArcTan\left(\frac{B \pm H_{Cb}}{c}\right)$$

to both ascending and descending branches of the hysteresis loop. Here M(B) is the magnetisation generated by a magnetic field B, M_S is the saturation magnetisation, H_C is the coercive force and c is a scaling constant. Measurement of H_{CR} from the backfield was not done for practical reasons. Instead, an estimation was attained by numerically finding the field at the maximum of the derivative of ΔM curve (Jackson et al., 1990).

2.4. Chemical analyses

Chemical analyses were performed in the accredited laboratory AcmeLabs in Canada for all samples for concentrations of Al, Ba, Cd, Co, Cr, Cu, Fe, Mn, Mo, Ni, Sb, Sr, Ti, V, W and Zn. The method applied was VG101 that uses 1 g split digested in HNO_2 then Aqua Regia after which, samples were analysed by inductively coupled plasma mass spectrometry (ICP-MS). The acceptability of results was ensured by the standard ratification method that uses two procedural blanks, two reference materials (STD CDV-1 and STD V16) and two QC protocol sample duplicates. The analysed control (n = 2) and background samples from Turku (n = 3) and Helsinki (n = 3) were calculated for average concentrations and then deducted from the original raw moss data (Table 2).

2.5. Data analysis

Statistical analyses were conducted using IBM SPSS Statistics version 27. The normality for all the data including mass-specific magnetic susceptibility (χ), saturation magnetisation (M_S) and element concentrations were tested with the Shapiro-Wilk test. None of the tested variables were normally distributed and therefore, Spearman's rank correlation coefficient was applied in the correlation between magnetic, element and height parameters.

2.6. OSPM modelling input data

2.6.1. Meteorological data

Meteorological data for Aninkaistenkatu, was received from the Finnish Meteorological Institution (FMI) weather station at Artukainen, Turku (5.10 km from study site to W), where air temperature is measured at height of 2 m, precipitation at a height of 1.5 m, and wind speed at a height of 23 m. For Runeberginkatu, the data was provided by the FMI weather station at Kaisaniemi, Helsinki (1.25 km from study site to ESE), where air temperature is measured at a height of 2 m, precipitation at a height of 1.5 m, and wind speed at a height of 31 m.

2.6.2. Background data

At Aninkaistenkatu the hourly average time series of PM_{10} concentrations (μg/m^3) for the background input data were acquired from the Raisio center monitoring station (6.60 km from the study site to NW) at a height of 3 m nearby a busy street (Turku, 2016). At Runeberginkatu the hourly average time series of PM_{10} concentrations (μg/m3) for the background input data were acquired from the urban background monitoring station in Kallio (1.90 km from study site to NE), operated by Helsinki Region Environmental Services (HSY). Kallio measurements were done at the height of 4 m.

Background data used in OSPM should be measured at the roof level close to the studied street section. Thus, the use of background measurements far from the study location and the preferred measurement height may cause some uncertainty in modelling e.g., local emissions in PM concentrations.

2.6.3. Traffic speed

The average travel speed or its variation over time in Aninkaistenkatu or nearby street in Turku was not available. Hence, the speed limit of 50 km/h was used as a travel speed value for all hours. This is not

the ideal, as it is too high during daytimes especially peak hours. The average weekday travel speed in Runeberginkatu is 27 km/h. The average weekday travel speed is based on estimations in Runeberginkatu in 2011 (Hellman, 2011). The variation of travel speed over time is based on Hellman (2011) and a monitoring campaign conducted by the city of Helsinki at Runebergin-katu in 2004. The travel speed data is the same for all vehicle types.

2.6.4. Traffic volume

Annual traffic volume in Aninkaistenkatu was ca. 21 000 veh/day based on traffic counts by Turku Environment Division in 2014. The share of different vehicle types within the whole traffic (Table 3) is based on estimates of the HDV share 2% in Aninkaistenkatu, assumed to be primarily buses, and the share of different vehicle types in LIPASTO mileage data of Turku in 2016 (Eckhardt, 2017, 2018). Hourly and day-of-week variation of traffic volume is based on Turku Environment Division traffic counts in Ratapihankatu, approximately 900 m west from the Aninkaistenkatu study site. The monthly variation of traffic volume in Turku was not available.

The annual average weekday traffic volume in Runeberginkatu was ca. 17 500 veh/day. The share of different vehicle types within the whole traffic is presented in Table 3. Hourly variation of traffic volume on weekdays is based on traffic counts on Wednesday August 17, 2016 at Runeberginkatu. Day-of-week and monthly variation of traffic volume are based on estimations in so called "Niemen raja" traffic flow counting line at the centre of Helsinki and on eight automated traffic counting points in Helsinki, respectively. The traffic volume data for Runeberginkatu is mainly based on Blomqvist and Salermo (2017) report on the development of traffic volume in Helsinki in 2016.

2.6.5. Exhaust emissions

We have used PM exhaust emission factors (g/km/veh) according to LIPASTO (Eckhardt, 2018). The LIPASTO emission factors are defined for different vehicle types (passenger cars, vans, buses and lorries no trailer) with constant "street" categorised speed in Turku and Helsinki (Table 4). Thus, we did not use speed-dependent functions for emission factors. In Aninkaistenkatu, all HDV's were assumed to be buses, and no emission factors for lorries were used.

2.6.6. Non-exhaust emissions

The FORE model (Forecasting Of Road dust Emissions; Kauhaniemi et al., 2011; Omstedt et al., 2005) is used to model the non-exhaust emission factors. They are the product of emission factors and total vehicle volume on studied street. The FORE model requires various input data; the reference emission factors, hourly meteorological data, the roughness length, the share of studded tyres, and the date and time of street sanding.

The influence of terrain on wind is determined by roughness length, which is necessary for the evaluation of evaporation (Omstedt et al., 2005). In this study, the roughness length was derived visually from the height of the buildings and open areas near street segment. A roughness length value of 1.0 m and 1.5 m was obtained for Aninkaistenkatu and Runeberginkatu, respectively.

The transition from summer to winter tyres, both in Runeberginkatu and Aninkaistenkatu, is based on weekly counting of vehicles with studded tyres in Helsinki (REDUST, 2014). The maximum annual share of vehicles using studded tyres is 80 % (Kupiainen, 2007). Thus, the assumed studded tyre share increases from 43.3% to 80% during the study period in Runeberginkatu and Aninkaistenkatu.

The sanding dates used in all cases were modelled by FORE based on meteorological conditions. In total 9 sanding events occurred during the study period at both locations. As no information of the sanding hours were available, sanding was assumed to occur at 6 a.m. at both sites. The reference emission factors for sanding period (Oct–May) are 150 (μg/m/veh) for PM2.5 and 1200 (μg/m/veh) for PM_{10} (Omstedt et al., 2005).

Table 3
The share of vehicle types within whole traffic in Aninkaistenkatu and Runeberginkatu.

Vehicle type	Aninkaistenkatu	Runeberginkatu
pCars	0.86	0.8
Vans	0.12	0.11
Busses	0.02	0.07
Lorries no trailer	0	0.02

Table 4
PM emission factors (g/km/veh) in "streets" in Turku and Helsinki, according to LIPASTO (Eckhardt, 2018; Eckhardt, 2017, respectively).

Vehicle type	PM eef Aninkaistenkatu	PM eef Runeberginkatu
pCars	0.01	0.009
Vans	0.08	0.08
Busses	0.05	0.09
Lorries no trailer	0	0.07

2.6.7. OSPM model

The street canyon dispersion model OSPM (Operational Street Pollution Model; Berkowicz, 2000) is a combination of Gaussian plume model and an empirical box model. The input data required includes time series of traffic, emissions, meteorology, and background concentration, as well as street configuration data. In the model, turbulence caused by traffic depends on travel speed and traffic volume of light and heavy vehicles. Additionally, to illustrate the local PM emissions street increment concentrations were calculated by subtracting background concentrations from OSPM modelled concentrations.

At both study locations the building heights, nearby parks and trees and street crossings needed to be considered in the building height exceptions, because they are located less than 200 m from the receptor points. Otherwise, the OSPM model will assume that the row of buildings continues over a very large distance (Berkowicz et al., 2003).

2.7. Large eddy simulation

Large eddy simulation (LES) is a computational approach that allows one to obtain time-resolved and fully three-dimensional information on the wind field (see e.g. Pope, 2000). In the present work, we have utilized earlier LES results on the flow past Turku to explain the characteristics of the street canyon winds. The simulation was performed for a case of strictly neutral stratification and the flow was driven using a constant pressure gradient for a several different wind directions. In addition to orographic features, the effect of buildings and vegetation to the flow were considered with spatial resolution down to 4 m. The simulations were carried out using the PALM model (Maronga et al. 2015, 2020) on the Puhti supercomputer of CSC – IT center for sciende Ltd. Further details on the simulation approach and the case set-up can be found from Keskinen et al. (2023).

3. Results

3.1. Magnetic susceptibility

The mass-specific magnetic susceptibilities varied between 43.45×10^{-8} m^3 kg^{-1} and 21.10×10^{-8} m^3 kg^{-1} at the Aninkaistenkatu street canyon, and 65.75×10^{-8} m^3 kg^{-1} and 11.25×10^{-8} m^3 kg^{-1} at the Runeberginkatu street canyon. The magnetic susceptibility values at Aninkaistenkatu north and south end were 27.90×10^{-8} m^3 kg^{-1} and 31.45×10^{-8} m^3 kg^{-1} and at Runeberginkatu north and south end 10.75×10^{-8} m^3 kg^{-1} and 13.50×10^{-8} m^3 kg^{-1}, respectively (Table 5). The highest magnetic susceptibility values were found on the eastern wall of Aninkaistenkatu at the height of 3 m and on the western wall of Runeberginkatu at the height of 3 m. At Aninkaistenkatu, the magnetic

Table 5
Summary of statistics for mass-specific magnetic susceptibility (χ x $10^{-8}m^3kg^{-1}$), saturation magnetisation (MS) and heavy metal consentreations (mg kg^{-1}) at different heights (3, 6, 9, 12 m) and on western (w) and eastern (e) sides at Aninkaistenkatu and Runeberginkatu.

	χ	M_S	Al	Ba	Cd	Co	Cr	Cu
Aninkaistenkatu								
12 m w/e	21.25/32.80	8.55/25.42	550/750	9.57/15.67	0.03/0.03	1.09/1.86	3.50/5.00	16.10/25.79
9 m w/e	28.75/32.55	17.39/24.39	750/850	12.17/14.17	0.04/0.02	1.37/1.64	4.40/4.60	19.88/20.30
6 m w/e	22.40/40.85	15.21/38.98	650/1150	10.47/18.97	0.05/0.02	1.08/2.15	4.10/6.40	17.37/28.06
3 m w/e	21.10/43.45	16.87/43.66	650/1250	8.67/18.77	0.05/0.02	1.32/2.05	4.00/6.00	15.18/24.82
North	27.90	20.67	750	13.57	0.02	1.67	4.90	20.25
South	31.45	23.41	850	14.17	0.02	1.53	4.60	22.42
Runeberginkatu								
12 m w/e	27.25/11.25	13.75/5.16	533/233	12.30/8.60	0.01/0.01	0.77/0.32	2.70/1.10	26.26/12.85
9 m w/e	35.70/12.80	24.90/4.73	833/333	16.60/9.50	0.01/0.01	0.93/0.72	4.20/1.50	34.97/15.10
6 m w/e	33.65/13.85	21.82/5.49	733/333	15.30/10.00	0.01/0.01	0.99/0.48	3.60/1.20	29.98/16.05
3 m w/e	65.75/21.45	48.80/5.42	1333/533	25.20/12.00	0.01/0.01	1.60/0.58	6.60/2.10	50.37/18.45
North	10.75	4.44	333	6.40	0.01	0.34	1.10	10.97
South	13.50	4.41	433	8.00	0.01	0.46	1.70	14.85

susceptibility values varied at different altitudes and a non-monotonic trend with altitude is shown on both sides of the street. This is also the case at the western side of Runerginkatu, but on the eastern side, the magnetic susceptibility values display a decreasing monotonic trend with altitude. On the western side of Aninkaistenkatu the Magnetic susceptibility profile is quite flat and the maximum value is reached at the height of 9 m. This is a direct consequence of the turbulent structure in the Aninkaistenkatu street canyon, with very strong and spatially irregular upward flows in the western side during westerly winds. This is discussed in more detail later in the paper. Mass-specific susceptibility values showed no marked dependence towards the increase of height except on the eastern side of Runeberginkatu. Our results show a different outcome in comparison with the observations of Lazić et al. (2016) who found an unambiguous agreement with OSPM modelled PM_{10} concentrations and moss bag element concentrations between vertical sample heights of 4 m and 16 m in all five street canyon sites. This might simply be due to a higher sampling quantity at different vertical intervals.

3.2. Magnetic mineralogy

Hysteresis characteristics of the samples exhibit thin loop curves and rapid saturation at 0.2–0.3 T (Fig. 2). H_C and H_{CR} values for Aninkaistenkatu range between 3.59 - 4.12 mT and 36.20–39.26 mT (derivative DeltaM), whereas for Runeberginkatu 4.07–4.99 mT and 33.86–37.32 mT (derivative DeltaM), respectively (Table 6). The slightly slanted shape of the hysteresis curves might refer to presence of SP particles, which give no hysteresis at all. SP particles have been associated with magnetic particles from traffic (e.g. Sagnotti et al., 2006; Chaparro et al., 2020; Muxworthy et al., 2022). The grain sizes of the magnetic particles were investigated using the hysteresis parameter ratios of M_{RS}/M_S and H_{CR}/H_C (Dunlop, 2002). The Day plot distribution of the hysteresis ratios are located in an area moving from the pseudo-single-domain (PSD) region (1–15 μm) (Dunlop, 2021) towards the theoretical mixing line for superparamagnetic (SP < 0.03 μm) SP-PSD grains (Dekkers, 1997) but closer to the boundary for small multi-domain (MD) grains (Dunlop, 2002) (Fig. 3). Dunlop states that data plots within this area are difficult to interpret but our data with mean H_{CR} value 36.16 mT might refer to broad grain-size distributions within PSD-stable SD-SP range (Fig. 3). Furthermore, the domain states plot similarly to Muxworthy et al., 2022 where the values locate above the MD region suggesting grain size differences in the magnetic PM. This suggests to a mixture of PSD and MD with the presence of SP particles.

3.3. Elemental concentrations

Chemical analysis (n = 28) included eight control and background samples. The element abundance orders for Aninkaistenkatu and Runeberginkatu were Fe > Al > Ti > Zn > Mn > Cu > Ba > W > V > Cr > Sr > Ni > Co > Sb > Mo > Cd and Fe > Al > Zn > Ti > Mn > Cu > Ba > Sr > V > Cr > W > Sb > Ni > Co > Mo > Cd, respectively (Table 5). The abundance orders were different between Aninkaistenkatu and Runeberginkatu as Ti and Zn interchanged their positions and W, Sr, Ni, Sb and Co have slightly different positions, also the concentrations of W, V and Cr were higher at Aninkaistenkatu. The highest element concentrations of Fe, Al, Ti, Zn, Mn, Cu and Ba were found on both the eastern side of Aninkaistenkatu and on the western side of Runeberginkatu at the heights of 3 m and 6 m.

3.4. OSPM modelling

At Aninkaistenkatu street canyon the OSPM model estimated the western face to have higher concentrations of PM compared to the eastern face (Table 7). The prevailing wind directions fluctuated in a rather wide spectrum during the sample period. The winds blew mostly nearly perpendicular to the direction of the street canyon from S-NW-directions, nevertheless occasionally the prevailing winds blew parallel from SE and NW-NNW-directions.

At the Runeberginkatu street canyon the OSPM model estimated the western face to have higher concentrations of PM compared to the eastern face (Table 7). Most of the time the winds blew perpendicular to the direction of the street canyon from the directions between SSW and N. However, occasionally there were strong winds from the opposite NE direction.

As expected, the OSPM model naturally showed monotonically decreasing concentrations with increasing altitude on both faces of the street canyon at both study sites (Table 7). The simulated daily average concentration time series for PM_{10} on both sides of the Aninkaistenkatu and Runeberginkatu and the observed concentrations from background monitoring stations are shown in Figs. 4 and 5.

3.5. Correlations

According to the Spearman's rank order correlation coefficient there was a strong significant correlation ($\rho < 0.01$) between χ, M_S and most heavy metals, excluding Cd, Zn and ($\rho < 0.05$) correlation between M_S and Sb (Table 8). There were no significant correlations between height (3 m, 6 m, 9 m and 12 m) and the values of χ, M_S or concentrations of heavy metals.

Fe	Mn	Mo	Ni	Sb	Sr	Ti	V	W	Zn
Aninkaistenkatu									
1110/1730	19/34	0.51/0.85	1.23/1.93	1.07/1.68	2.63/4.63	56.67/83.67	4.00/6.00	5.35/9.25	67.03/47.23
1480/1650	30/29	0.66/0.69	1.63/1.73	1.29/1.37	3.53/4.33	74.67/84.67	5.00/5.00	6.95/8.65	44.23/29.33
1350/2340	22/46	0.58/0.93	1.33/2.33	1.10/1.79	3.03/5.33	70.67/122.67	5.00/7.00	6.25/11.85	22.43/41.93
1210/2350	22/39	0.45/0.85	1.43/2.13	0.86/1.58	2.73/5.33	64.67/134.67	4.00/7.00	6.05/12.05	35.33/36.23
1670	30	0.70	1.63	1.82	3.93	86.67	5.00	8.15	23.73
1670	30	0.73	1.63	1.48	3.83	82.67	5.00	8.25	41.23
Runeberginkatu									
1383/593	30/23	0.70/0.34	1.70/0.90	2.08/1.00	3.10/1.80	39.00/17.00	3.00/2.00	2.60/1.20	64.57/21.27
1903/743	38/23	0.93/0.41	2.20/1.10	2.70/1.24	4.30/2.00	56.00/21.00	5.00/2.00	3.80/1.40	68.47/62.97
1793/723	33/16	0.86/0.36	2.10/1.00	2.44/1.29	3.90/2.20	54.00/21.00	4.00/2.00	3.30/1.40	81.67/50.67
3093/1173	47/17	1.52/0.55	3.60/1.40	4.30/1.79	7.20/2.60	97.00/38.00	7.00/2.00	6.10/2.30	119.27/51.77
633	15	0.31	0.80	0.87	1.70	21.00	2.00	1.40	48.47
893	22	0.40	1.20	1.03	2.30	27.00	2.00	1.80	40.27

4. Discussion

Ferrimagnetic minerals are shown to characterize the magnetic properties of traffic emission particulates (Hunt et al., 1984; Lu et al., 2005; Salo et al., 2012; Chaparro et al., 2020; Muxworthy et al., 2022). In this study the exposed moss bags display narrow hysteresis loops with rapid saturations at 0.2–0.3 mT and low values of H_{CR}, which indicate the presence of low-coercivity ferrimagnetic minerals (Fig. 2). The mean H_{CR} value 36,16 mT is similar to those reported for anthropogenic magnetite (Chaparro et al., 2013, 2020; Gómez et al., 2021; Winkler

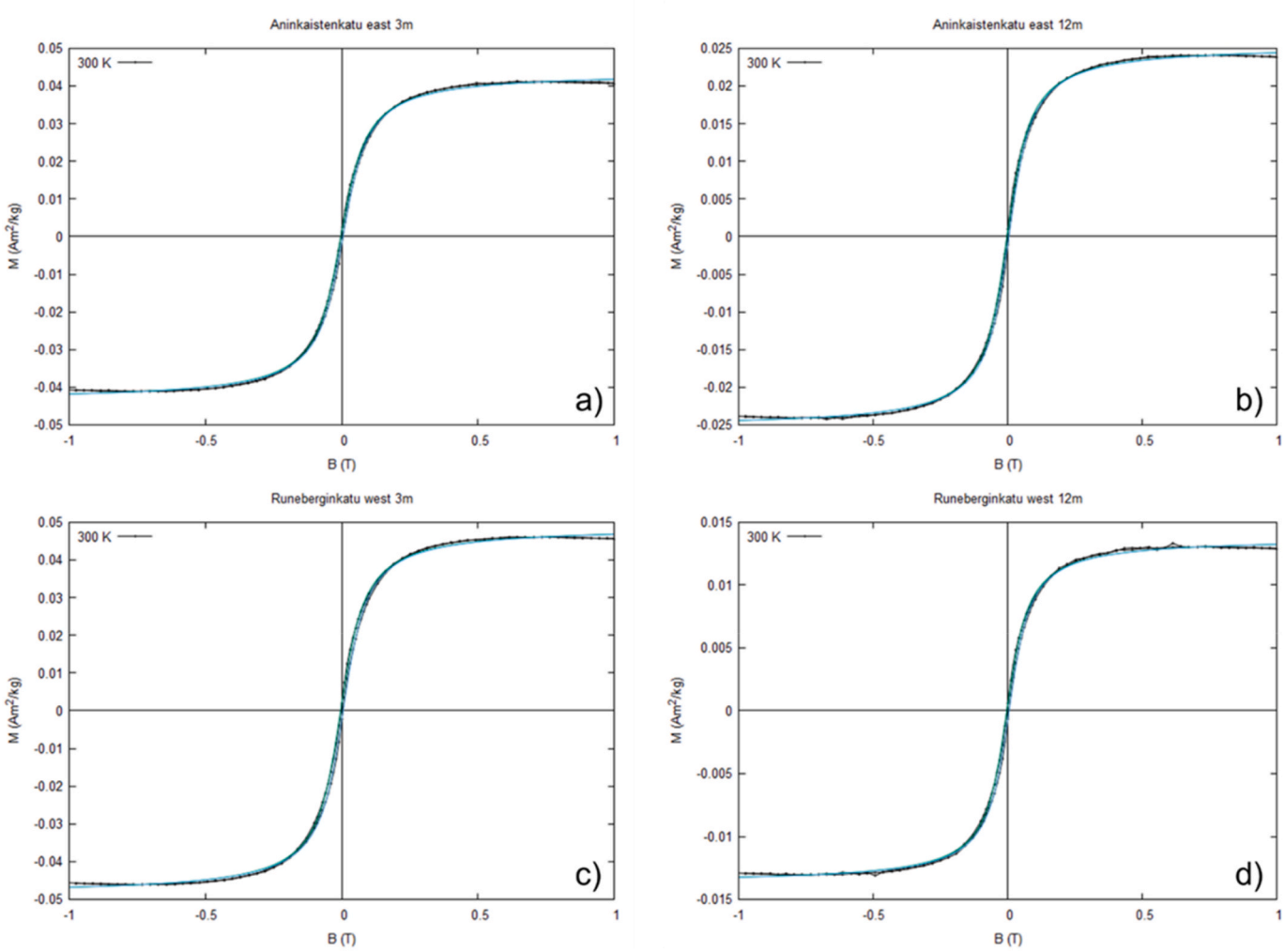

Fig. 2. Hysteresis loops of chosen samples at Aninkaistenkatu (a, b) and Runeberginkatu (c, d). Magnetic field B (T) illustrated on the x-axis and magnetisation M (Am^2/kg) on y-axis.

Table 6
Summary of saturation magnetisation (M_S ($mAm^2\ kg^{-1}$)), saturation remanence (M_{RS} ($mAm^2\ kg^{-1}$)), coercive force (H_C (mT)) and coercivity of remanence (H_{CR} (mT)) at different heights (3, 6, 9, 12 m) and on western (w) and eastern (e) sides at Aninkaistenkatu and Runeberginkatu.

	M_s	M_{rs}	H_c	H_{cr}
Aninkaistenkatu				
12 m w/e	8.55/25.42	0.35/0.94	4.09/3.65	36.81/36.20
9 m w/e	17.39/24.39	0.69/0.93	3.97/3.79	36.64/36.75
6 m w/e	15.21/38.98	0.55/1.47	3.59/3.89	36.62/38.06
3 m w/e	16.87/43.66	0.66/1.58	4.12/3.86	38.67/39.26
North	20.67	0.85	4.24	37.77
South	23.41	0.8	3.51	37.74
Runeberginkatu				
12 m w/e	13.75/5.16	0.62/0.26	4.17/4.60	33.86/34.01
9 m w/e	24.90/4.73	1.05/0.21	4.07/4.35	35.50/35.50
6 m w/e	21.82/5.49	0.95/0.29	4.23/4.99	35.72/34.44
3 m w/e	48.80/5.42	2.19/0.27	4.55/4.51	37.32/33.96
North	4.44	0.22	4.61	34.19
South	4.41	0.23	4.77	33.92

et al., 2019) and traffic emissions (Chaparro et al., 2020; Chaparro et al., 2023; Muxworthy et al., 2022; Sagnotti et al., 2006). In previous studies executed in Turku, magnetite was the primary low-coercivity ferrimagnetic mineral found in traffic related air pollution in Turku (Limo et al., 2018; Salo and Mäkinen, 2019). Pakkanen et al. (2003) found that in Helsinki at street level the traffic related concentrations of Ba, Th, Fe, Mn, Pb and Sb were dominant, and the roof top long range transport submicron particles were mainly composed of SO_4^{2-}, NH_4^+ Tl, As, K^+, Cd, B in every sampling period. Moreover, a very high correlation between Fe (magnetic PM) and Al (non-magnetic PM from soil and rock minerals) concentrations indicate that they originate from the same source, which in this case is street dust (Table 8). Furthermore, regarding to the recent emission model inventories executed for Turku and Helsinki, the effect of industry or energy production in the PM concentrations within the two studied cities are very low (FMI, 2022a; FMI, 2022b). Therefore, it is reasonable to assume that the ferrimagnetic magnetite is the predominant magnetic mineral found in the moss bag samples in this study.

The hysteresis ratios most probably indicate mixture of different magnetic grain-sizes and the dominance of PM_{10} sized material but might also point to somewhat bimodal SP-PSD/MD grain-size distribution (Chaparro et al., 2020), where SP grains would be dominantly from traffic exhaust emissions and coarser grains from abrasion of metallic parts (Sagnotti et al., 2006). The data show conformity to earlier studies that involve magnetic PM properties in Turku (Limo et al., 2018; Salo and Mäkinen, 2019). In Finland, cars have studded tyres during the winter and traction sand is used for the streets, which generates ultrafine particles (<100 nm) and makes resuspension of road dust a strong PM source (Fussel et al., 2022). Furthermore, Tretiach et al. (2011) points out that moss bags predominantly entrap the PM fraction of <2.5 μm (78.8%) over the coarser fraction of 2.5–10 μm. According to Chaparro et al. (2020) most of the low-coercivity, magnetite-like Fe-rich particles derived from the traffic are <2.5 μm.

The highest element concentrations were displayed by Fe, Al, Ti, Zn, Mn, Cu and Ba and the abundance orders of these were almost identical in both street canyon locations (Table 5). The exact same elements had the highest concentrations in heavily trafficked street sections in Turku (Limo et al., 2018). These elements are highly abundant in the urban environments and can be related to various emissions from traffic (Adachi and Tainosho, 2004; Moreno et al., 2011; Ozaki et al., 2004) and crustal/road dust (Hueglin et al., 2005; Viana et al., 2006). All the measured elements share a strong correlation between χ and M_S except for Cd and Zn (Table 8). The concentrations of Cd were very low and therefore it is difficult to address its source to urban air. The source of Zn is commonly associated with tire wear particles (Baensch-Baltruschat et al., 2020; Napier et al., 2008), which might explain the unattached relation to Fe also described by Limo et al. (2018). A considerable difference between the study locations is that Runeberginkatu seemed to have significantly higher values of χ and concentrations of most elements. The traffic volumes are rather similar between the two locations, but the most substantial difference is a tramline, which runs in the middle of Runeberginkatu. According to van Laaten et al. (2021) tram

Table 7
The average concentrations of PM_{10} modelled by the OSPM and measured mass-specific magnetic susceptibilities (χ x $10^{-8} m^3 kg^{-1}$) at different heights (3, 6, 9, 12 m) and on western (w) and eastern (e) sides at Aninkaistenkatu and Runeberginkatu.

	PM_{10}	χ
Aninkaistenkatu		
12 m w/e	12.40/11.87	21.25/32.80
9 m w/e	13.51/12.64	28.75/32.55
6 m w/e	15.29/13.92	22.40/40.85
3 m w/e	18.44/16.21	21.10/43.45
	PM_{10}	χ
Runeberginkatu		
12 m w/e	12.99/12.69	27.25/11.25
9 m w/e	14.02/13.22	35.70/12.80
6 m w/e	16.36/14.21	33.65/13.85
3 m w/e	21.08/16.28	65.75/21.45

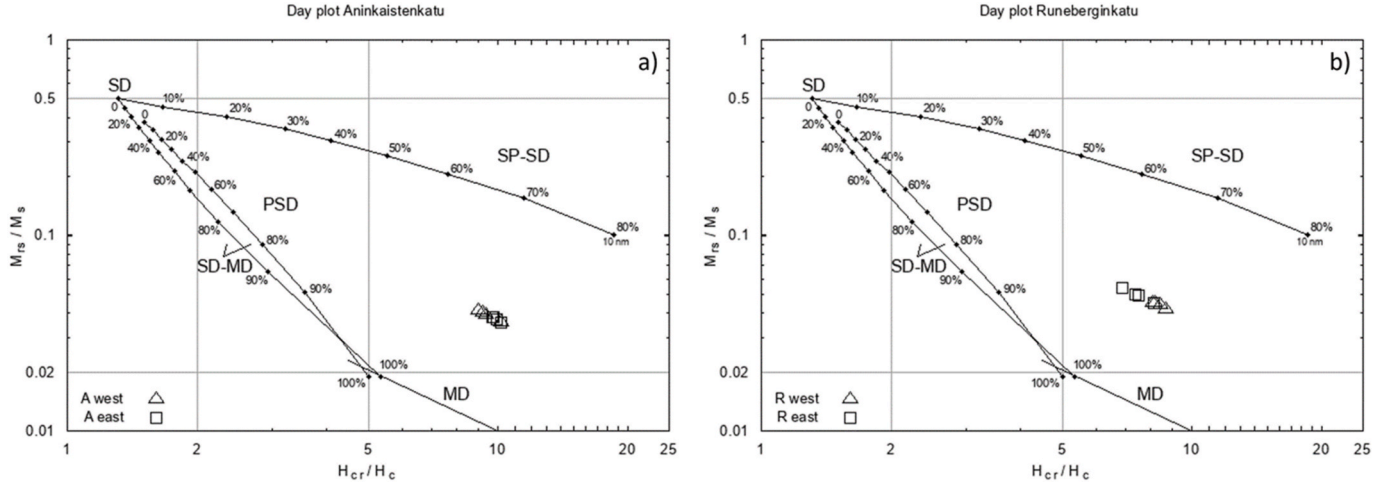

Fig. 3. Day plot diagrams of the ratios M_{RS}/M_S and H_{RC}/H_C of the samples for a) Aninkaistenkatu and b) Runeberginkatu. The boundaries for Single-domain (SD), superparamagnetic (SP), pseudo-single-domain (PSD) and multidomain (MD) grains and mixing lines as illustrated in Dunlop (2002).

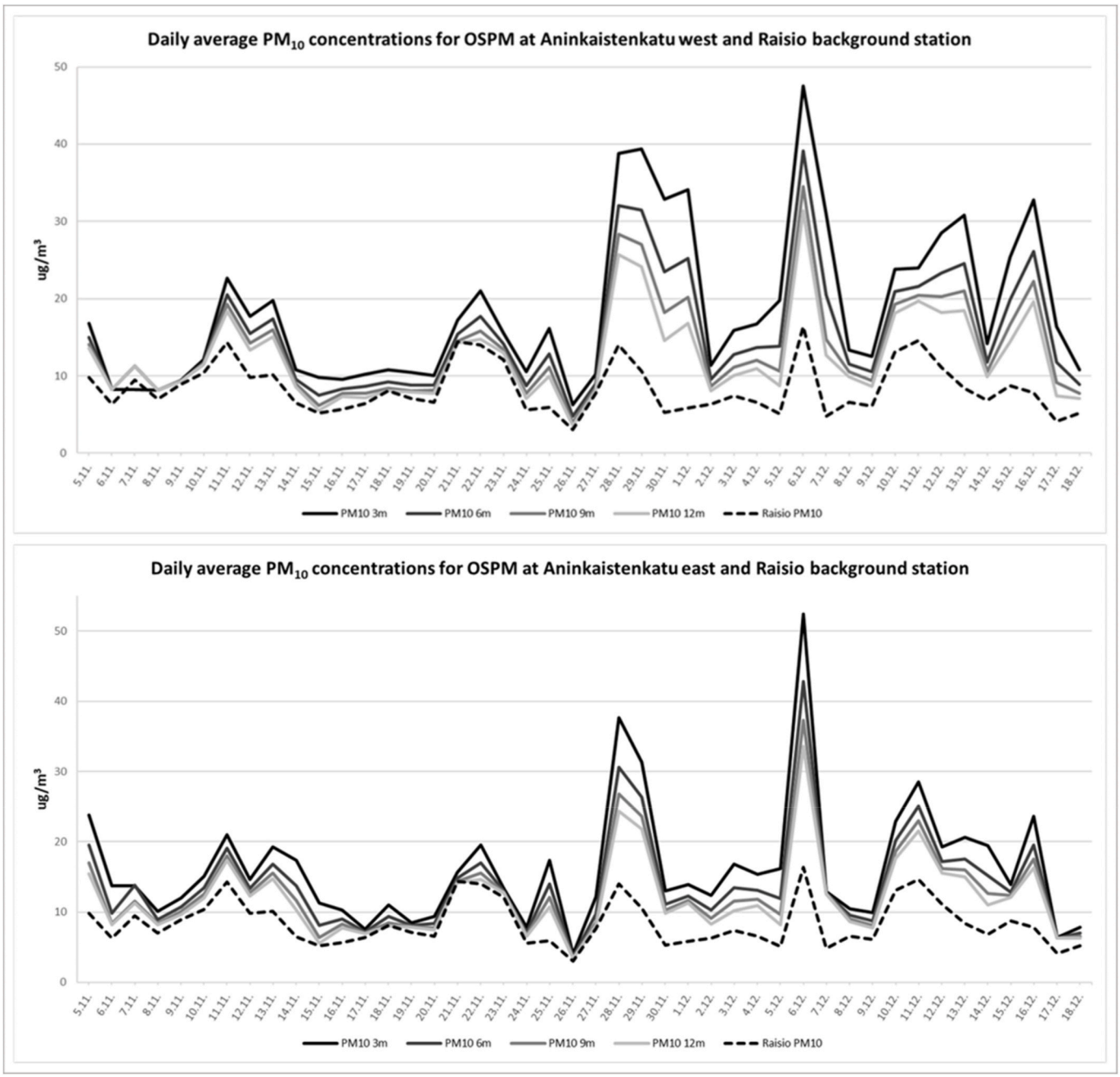

Fig. 4. Daily average concentrations of PM_{10} at Raisio background station and OSPM concentrations modelled at Aninkaistenkatu west (above) and east (below).

traffic might constitute a considerable source for elements in the local PM. Nevertheless, the strong correlation between Fe and the other elements show that iron is highly involved with the abundance of the other elements. Therefore, magnetic methods are a very useful tool in identifying traffic-induced iron oxides (magnetite) and related elements.

The highest values for magnetic susceptibilities χ were found at the height of 3 m on the eastern face of Aninkaistenkatu and on the western face of Runeberginkatu (Fig. 6). Therefore, the highest values of χ and elements observed on these street faces would suggest that they are the leeward sides against the prevailing wind direction over the roof top. The prevailing winds in Turku scatter along a wide range of directions (SE-NNW) and there are no obvious dominant prevailing winds perpendicular to the direction of the street canyon (Fig. 1). There are two distinct directions of high volume and high-speed winds from SE and NNW, which might dictate to the predominant vortex direction in the Aninkaistenkatu street canyon. However, the Artukainen weather station is ca. 5.1 km west from the location of Aninkaistenkatu street canyon and it is unclear how the urban geometry and the SW-NE orientated river valley affects the wind flow in relation to the sample site. In Helsinki the prevailing winds settle onto a narrower range (WSW-NW), but similarly to Turku, there are no obvious dominant prevailing winds perpendicular to the direction of the street canyon (Fig. 1). The vortex downwind in the street canyon is created on the windward side and upward wind vice versa on leeward side against the prevailing wind direction. Therefore, pollutants from the street level are first transported upwind and then upward on the leeward side (Baik and Kim, 2002).

The values of χ on the street canyon faces were non-monotonic in relation to increasing altitude except on the eastern side of Runeberginkatu where a decreasing monotonic trend could be observed (Fig. 6). This highly non-monotonic behaviour is best displayed on the western face of Aninkaistenkatu where the highest value of χ is reached

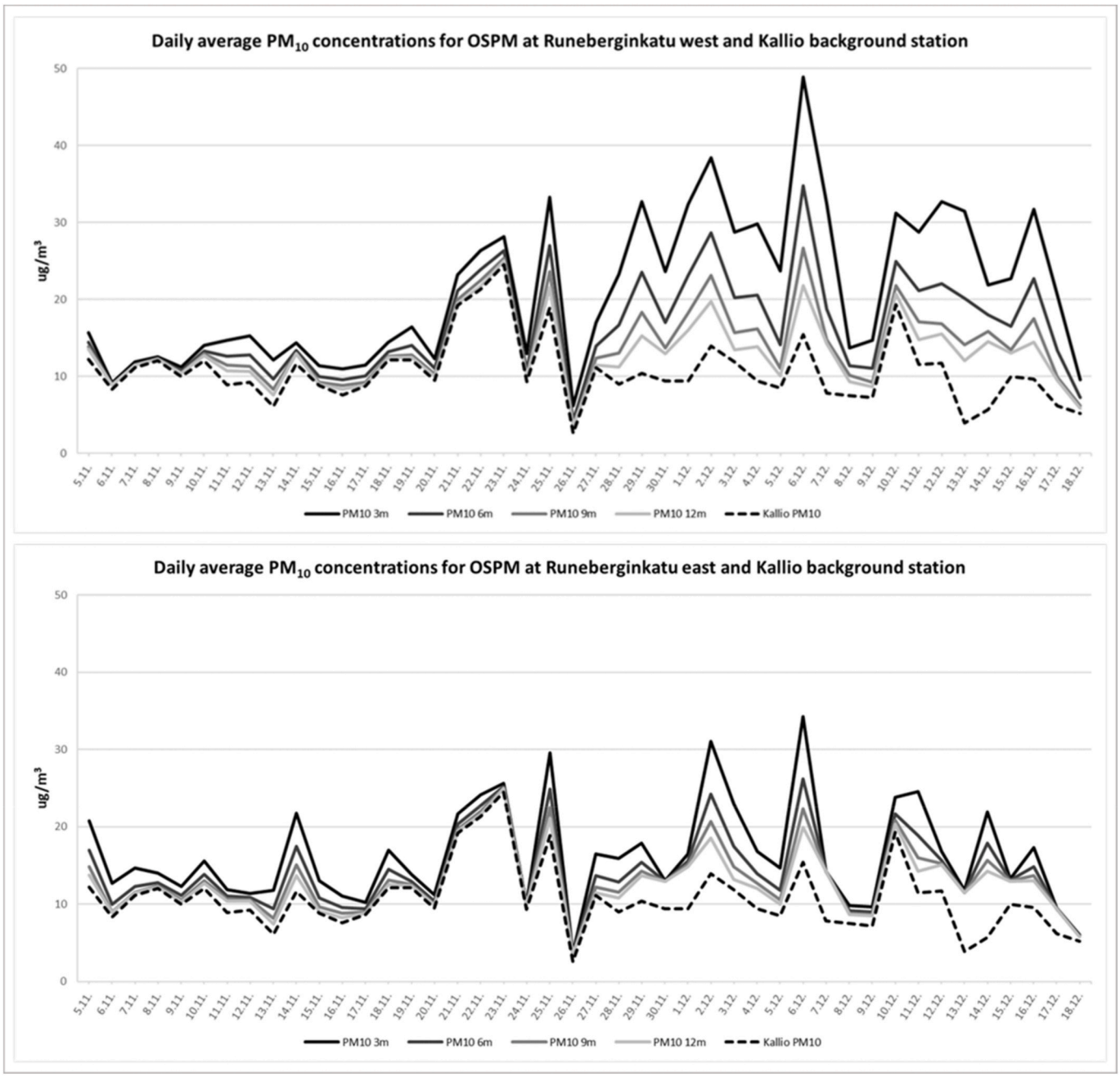

Fig. 5. Daily average concentrations of PM_{10} at Kallio background station and OSPM concentrations modelled at Runeberginkatu west (above) and east (below).

at the height of 9 m. Our results indicate that the highly coupled but irregular elevational distributions of magnetic PM within the street canyon was greatly influenced by the turbulent wind vortex. Nevertheless, the exact proportions of PM fractions in the magnetic PM are very difficult to determine. However, the dominant size fraction in our magnetic PM is closer to fine particulates ($PM_{2.5}$) within the PM_{10}, and the moss bags dominantly entrap $PM_{2.5}$ over the $PM_{2.5\text{-}10}$ fraction (Tretiach et al., 2011). Moreover, the elements that originate mainly from anthropogenic processes (e.g. traffic) are predominantly found in the $PM_{2.5}$ fraction and crustal elements on the other hand occur predominantly in the coarse $PM_{2.5\text{-}10}$ fraction (Hueglin et al., 2005; Slezakova et al., 2007) with the exception of kerbside locations where re-suspended mineral dust particles and mechanically generated particles prevail (Hueglin et al., 2005).

The results of the OSPM model at Runeberginkatu agree with the magnetic data in such that the predominant westerly winds dictate the direction of the wind vortex in the street canyon and the leeward side is the western face. Therefore, it is subject to higher concentrations and accumulation of PM than the eastern face. There is a considerable difference with the modelled PM concentrations between the leeward and windward faces and the equivalent magnetic susceptibility values even at each height level. This seems to indicate that the measurements catch the small-scale variation caused by the local traffic emissions very efficiently. On the contrary, the local traffic input in OSPM estimations can be achieved with street increment concentrations where background values have been removed. The street increment estimations emphasize the contrast in fluctuations of concentrations but here the overall trend in concentrations remains the same with estimations where the background values are included (Fig. 6). Furthermore, the OSPM also underestimates the irregular behaviour of the concentrations at different heights on the more polluted face, whereas the values of χ suggest a much more turbulent behaviour of the upwind in the vortex. This is a

Table 8
Summary of Spearman's rank order correlation coefficient (n = 20) for mass-specific magnetic susceptibility (χ x $10^{-8}m^3kg^{-1}$), saturation magnetisation (M_S), element concentrations and different heights (A, aninkaistenkatu; R, Runeberginkatu).

	χ	M_S	Al	Ba	Cd	Co	Cr	Cu	Fe	Mn	Mo	Ni	Sb	Sr	Ti	V	W	Zn
ρ X	1.000	0.938**	0.926**	0.974**	0.066	0.718**	0.876**	0.918**	0.988**	0.865**	0.965**	0.965**	0.763**	.0964**	0.781**	0.867**	0.705**	0.303
ρ Ms	0.938**	1.000	0.963**	0.888**	0.265	0.838**	0.947**	0.794**	0.953**	0.839**	0.875**	0.924**	0.563*	0.979**	0.879**	0.942**	0.814**	0.115
ρ Fe	0.988**	0.953**	0.940**	0.947**	0.113	0.747**	0.897**	0.894**	1.000	0.893**	0.959**	0.979**	0.722**	0.970**	0.799**	0.880**	0.723**	0.265
ρ A height	−0.098	−0.293	−0.346	−0.049	−0.3	−0.146	−0.195	0.098	−0.244	−0.221	0.025	−0.244	0.098	−0.221	−0.293	−0.203	−0.244	0.634
ρ R height	−0.439	−0.342	0.214	−0.439	0.000	−0.342	−0.390	−0.439	−0.390	−0.025	−0.390	−0.390	−0.439	−0.439	−0.417	−0.208	−0.417	−0.342

*Correlation is significant at 0.01-level.
**Correlation is significant at 0.05-level.

direct consequence of the simplifications made in handling the street canyon meteorology in OSPM. On the eastern face where the local emission do not dominate, the magnetic susceptibility data and the OSPM seem to follow similar vertical profile.

At Aninkaistenkatu the OSPM results and the magnetic data are not compatible. In the OSPM simulation the higher concentrations were estimated to accumulate on the opposite western face whereas the measured magnetic susceptibility values were higher on the eastern face. This implies that the actual prevailing wind directions may be different from the ones used as input data in the model. The different outcome may partly be caused by the fact that the meteorological data for the OSPM was obtained from the FMI weather station at Artukainen, which lies ca. 5.1 km away from the street canyon. Therefore, the roof level wind directions at the street canyon site might be different to the directions at the distant weather station.

Another major challenge for OSPM model in this location is the more complicated structure of the street canyon. The situation was further studied using wind data obtained with LES. The simulated vertical wind velocities at Aninkaisenkatu are shown in Fig. 7 For three different wind directions. A complex flow pattern is revealed by the simulations. Fig. 7 clearly illustrates that at the measurement location indicated by the circles, already a 30-degree difference in the driving wind direction can change the local wind pattern inside the street canyon completely. A weak street canyon vortex can be identified from the vertical velocities in the case of 195°and perhaps also for the 225° wind direction. At 255° wind, the measurement location does not display a clear vortex. It is thus obvious that the flow does not follow the assumptions of OSPM in all of the cases where the difference between driving wind directions changes even with ±30°.

Like in Runeberginkatu, the relative difference of the modelled concentrations of PM on the leeward and windward faces is much smaller than observed in the magnetic measurements, so this agrees with our earlier results stating that the values of χ are much more sensitive to local traffic emissions than the modelled PM concentrations. The problem of assuming a simple vortex in the street canyon is reflected by the inability to predict the irregular behaviour of concentration gradient at different heights on the street canyon sides. The values of χ and the preliminary flow modelling results suggest a much more complicated turbulent behaviour inside the street canyon than assumed by the OSPM model.

Further, also the sloping hill might have a significant influence on inhomogeneous emissions and deposition in a street canyon. Gidhagen et al. (2004) examined measured NO_X emissions and observed that vehicles running uphill had higher emissions than those running downhill (2.3 % slope). Furthermore, a similar tendency was observed for measured particles, though this was deemed quantitatively insufficient since only a single monitoring point was used to monitor particle numbers. They also noted that in the case of ultra-fine particles, the total number (ToN) emission factors are likely to double with temperatures below 0 °C. An increase in airborne ultra-fine metals (Fe, Cu, Ni, Mn and Zn) associated with cars accelerating and braking in winter conditions was observed by Cahill et al. (2014). According to Ottosen et al. (2015) the greatest impact on the inhomogeneous emissions on sloping street canyons was highest during near-parallel wind directions. Furthermore, emission factors for PM fluctuate considerably depending on a slope gradient. For example, at slope angles of +0.06 or −0.06, buses have considerably different in PM emission factors (EMEP/EEA). These factors cannot be considered in the OSPM model as it assumes homogeneous emissions over the street e.g. emissions separated by lane or direction cannot be taken into account. Consequently, emission from uphill and downhill driving cannot be separated either. Aninkaistenkatu has a slope of 6.9 % (Fig. 6), and during the sampling period the prevailing wind direction was quite frequently near parallel to the street canyon and the average temperature −0.67 °C (Fig. 1). It is likely that the above-mentioned factors influenced the difference in contradicting results between the OSPM and the moss bag technique at

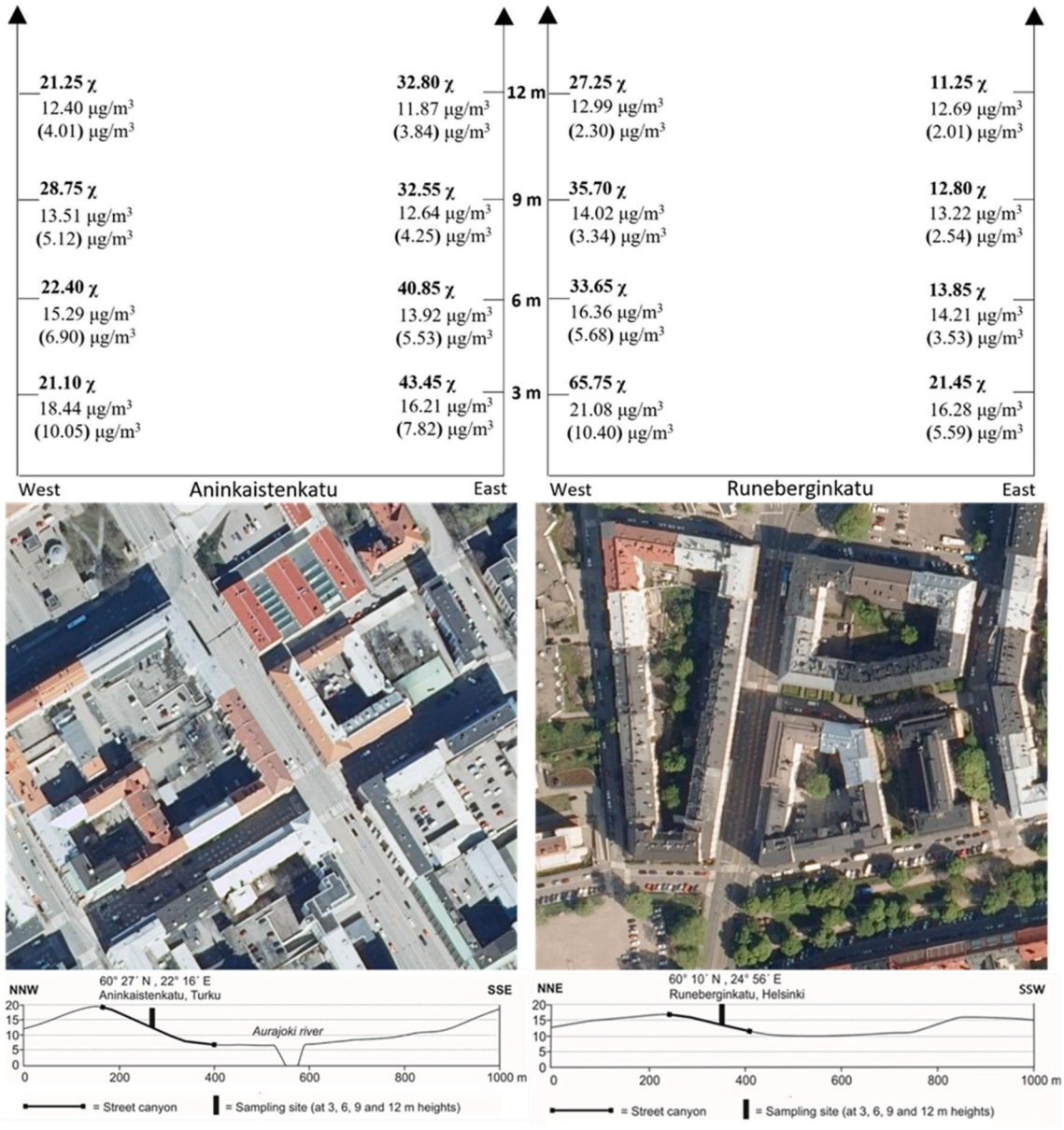

Fig. 6. Height distributions of mass-specific magnetic susceptibilities (χ x 10^{-8} m^3 kg^{-1}), OSPM modelled average concentrations of PM_{10} (µg/m^3) and street increment concentrations (in brackets) and height profiles of the street canyon sections at Aninkaistenkatu and Runeberginkatu. National Land Survey of Finland, https://asiointi.maanmittauslaitos.fi/karttapaikka/.

Aninkaistenkatu to a large extent.

Our study exhibits the versatility of moss bag technique as an excellent tool to assess the monitoring and modelling of airborne urban pollution. It offers a good spatial resolution for data collection with long sampling periods at a multitude of various sites. Therefore, the technique allows a variety of sampling strategies and exposure periods. The method provides a cost-effective tool to study the concentration of pollution from wide variety of sources.

5. Conclusions

Moss bag magnetic measurements and supporting chemical analyses of this study clearly demonstrate that traffic causes a significant input of low-coercivity ferrimagnetic minerals and heavy metals in busy street canyons. The magnetic PM is composed of magnetite and a mixture of PSD/MD grains with the presence of SP particles. Fe, Al, Ti, Zn, Mn, Cu and Ba had the highest element abundances at both street canyon locations. Magnetic measurements demonstrated the predominant wind vortex direction within the street canyons with significantly higher magnetic susceptibility values on the leeward sides, whereas the OSPM model predicted a much flatter PM concentration distribution inside the street canyon, which indicates that only a part of the modelled PM mass contributed to the magnetic susceptibility. The OSPM model predicted simple Gaussian dilution of PM concentrations with increasing height whereas for magnetic susceptibility the measured vertical profiles did not follow the simplified OSPM modelling, indicating much more complicated local wind fields inside the street canyon. The results between the OSPM model and magnetic measurements in Turku were incompatible and we argue that the meteorological input data for modelling should have been obtained in situ to strengthen the model. In addition, we believe that the high slope angle, the complicated structure (crossing street in the middle of the canyon) and the winter conditions might have contributed to the inhomogeneous emissions and concentrations at the street canyon in Turku. Our study also clearly illustrates that moss bags and magnetic biomonitoring together produce an effective economical method to assist in understanding and interpreting the

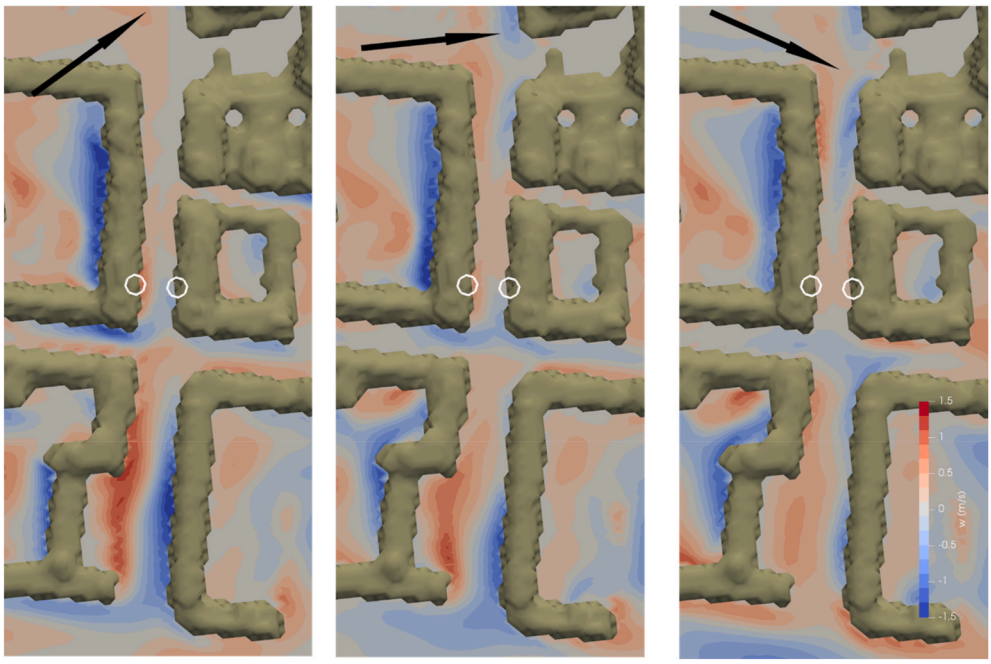

Fig. 7. Vertical wind velocity from LES at Aninkaisenkatu street canyon for driving wind directions of 195°, 225°, and 255° degrees. (red = upward flow, blue = downward flow). Driving wind direction is shown using the black arrow. Measurement locations on the sides of the street canyon are indicated with white circles.

concentration distributions and evaluating air quality modelling results in urban areas.

CRediT authorship contribution statement

Jukka Limo: Conceptualization, Data curation, Formal analysis, Funding acquisition, Investigation, Methodology, Resources, Supervision, Visualization, Writing – original draft, Writing – review & editing. **Mari Kauhaniemi:** Data curation, Formal analysis, Methodology, Software, Writing – original draft, Writing – review & editing. **Petriina Paturi:** Data curation, Formal analysis, Methodology, Resources, Software, Writing – review & editing. **Jukka-Pekka Keskinen:** Formal analysis, Methodology, Software, Writing – original draft, Writing – review & editing. **Ari Karppinen:** Conceptualization, Formal analysis, Methodology, Resources, Supervision, Writing – review & editing. **Joni Mäkinen:** Conceptualization, Methodology, Resources, Supervision, Writing – review & editing.

Declaration of competing interest

The authors declare that they have no known competing financial interests or personal relationships that could have appeared to influence the work reported in this paper.

Data availability

Data will be made available on request.

Acknowledgements

This study was funded by the Finnish Cultural Foundation (grant 00190638) and the Department of Geography and Geology, University of Turku. We would like to thank Kaarinan Rantakulman and Tammisalon voluntary fire brigades for logistical support in the field, and Aninkaistenkatu 5, Aninkaistenkatu 10, Runeberginkatu 36 and Runeberginkatu 49 housing cooperatives for allowing us to utilize their property. We would like to thank Turku infrastructure services and Helsinki city engineer's office for permitting us to momentarily distract city street logistics. In addition, we would like to thank Turku public authorities Miika Meretoja and Kimmo Knaapi for assistance and Camilla Gustafsson for providing comments on the manuscript. We also wish to acknowledge CSC – IT Center for Science, Finland for computational resources used in the LES. The LES was carried out as a part of the RESPONSE project. This programme has received funding from the European Environment Agency, 2013a research and innovation programme under Grant Agreement no 957751.

References

Adachi, K., Tainosho, Y., 2004. Characterization of heavy metal particles embedded in tire dust. Environ. Int. 30, 1009–1017.
Ares, A., Aboal, J., Carballeira, J.A., Fernández, J.A., 2015. Do moss bags containing devitalized Sphagnum denticulatum reflect heavy metal concentrations in bulk deposition? Ecol. Indicat. 50, 90–98.
Assael, M.J., Delaki, M., Kakosimos, K.E., 2008. Applying the OSPM model to the calculation of PM10 concentration levels in the historical centre of the city of Thessaloniki. Atmos. Environ. 42, 65–77.
Baensch-Baltruschat, B., Kocher, B., Stock, F., Reifferscheid, G., 2020. Tyre and road particles (TRWP) – a review of generation, properties, emissions, human health risk, ecotoxicity, and fate in the environment. Science of the Total Enviironment 733, 137823.
Baik, J.-J., Kim, J.-J., 2002. On the escape of pollutants from urban street canyons. Atmos. Environ. 36, 527–536.
Berkowicz, R., 2000. Ospm – a parameterised street pollution model. Environ. Monit. Assess. 65, 323–331.
Berkowicz, R., Olesen, R.H., Jensen, S.S., 2003. WinOSPM Operational Street Pollution Model Draft – March 2003, NERI Technical Report No. &&, Ministry of the Environment. National Environmental Research Institute.
Blomqvist, Kostiainen, Salermo, Yli-Seppälä, 2017. Liikenteen Kehitys Helsingissä 2016, Helsingin Kaupungin Kaupunkiympäristön Julkaisuja 2017:5, Syyskuu 2017, p. 61 (in Finnish). https://www.hel.fi/static/liitteet/kaupunkiymparisto/julkaisut/julkaisut/julkaisu-05-17.pdf.
Britter, R.E., Hanna, S.R., 2003. Flow and dispersion in urban areas. Annu. Rev. Fluid Mech. 35, 469–496.
Brown, D.H., Bates, J.W., 1990. Bryophytes and nutrient cycling. Bot. J. Linn. Soc. 104, 129–147.
Cahill, T.A., Barnes, D.E., Spada, N.J., 2014. Seasonal variability of ultra-fine metals downwind of a heavily travelled secondary road. Atmos. Environ. 94, 173–179.
Castañeda-Miranda, A.G., Chaparro, M.A.E., Pacheco-Castro, A., Chaparro, M.A.E., Böhnel, H.N., 2020. Environ. Monit. Assess. 192, 382.
Caton, F., Britter, R.E., Dalziel, S., 2003. Dispersion mechanics in a street canyon. Atmos. Environ. 37, 693–702.
Chaparro, M.A.E., Lavornia, J.M., Chaparro, M.A.E., Sinito, A.M., 2013. Biomonitors of urban air pollution: magnetic studies and SEM observations of corticolous foliose

and microfoliose lichens and their suitability for magnetic monitoring. Environ. Pollut. 172, 61–69.
Chaparro, M.A.E., Chaparro, M.A.E., Castañeda-Miranda, A.G., Marié, D.C., Garguilo, J. D., Lavornia, J.M., Natal, M., Böhnel, H.N., 2020. Fine air pollution particles trapped by street tree barks: in situ magnetic biomonitoring. Environ. Pollut. 266, 115229.
Chaparro, M.A.E., Buitrago Posada, D., Chaparro, M.A.E., Molinari, D., Chiavarino, L., Alba, B., Marié, D.C., Natal, M., Böhnel, H.N., Vaira, M., 2023. Urban and suburban's airborne magnetic particles accumulated on *Tillandsia capillaris*. Sci. Total Environ. 907, 167890.
De Nicola, F., Murena, F., Costagliola, M.A., Alfani, A., Baldantoni, D., Prati, M.V., Sessa, L., Spagnuolo, V., Giordano, S., 2013. A multi-approach monitoring of particulate matter, metals and PAHs in an urban street canyon. Environ. Sci. Pollut. Control Ser. 20, 4969–4979.
De Paul, F.T., Sheih, C.M., 1985. A tracer study of dispersion in an urban street canyon. Atmos. Environ. 19 (4), 555–559.
De Paul, F.T., Sheih, C.M., 1986. Measurements of wind velocities in a street canyon. Atmos. Environ. 20 (3), 455–459.
Dekkers, M.J., 1997. Environmental magnetism: an introduction. Geol. Mijnbouw 76 (1), 163–182.
Di Palma, A., GonzálezA, G., Adamo, P., Giordano, S., Reski, R., Pokrovsy, O.S., 2019. Biosurface properties and lead absorption in a clone of Sphagnum palustre (Mosses): towards a unified protocol of biomonitoring of airborne heavy metal pollution. Chemosphere 236, 124375.
Dunlop, D.J., 2002. Theory and application of the Day plot (M_{RS}/M_S versus H_{CR}/H_C) 2. Application to data for rocks, sediments, and soils. J. Geophys. Res. 107 (B3), 2056.
Dunlop, D.J., 2021. Magnetic hysteresis of magnetite at high temperatures: grain size variation. Geophys. J. Int. 226, 816–827.
Eckhardt, J., 2017. Suomen Tieliikenteen Päästöt Ja Energiankäyttö Kunnittain Vuonna 2016, VTT LIISA Laskentajärjestelmä, kunnat2016.Xlsx updated 27.6.2017. http://lipasto.vtt.fi/liisa/kunnat.htm. downloaded 11.1.2018.
Eckhardt, J., 2018. Suomen Tieliikenteen Päästöt Ja Energiankäyttö Kunnittain Vuonna 2016, VTT LIISA Laskentajärjestelmä, kunnat2016.Xlsx updated 14.11.2018. http://lipasto.vtt.fi/liisa/kunnat.htm. downloaded 25.3.2019.
EMEP/EEA Air Pollutant Emission Inventory Guidebook 2019 – Update Oct. 2021. EEA Report No 13/2019. European Environment Agency, Denmark. ISBN 978-92-9480-098-5.
Eskridge, R.E., Rao, S.T., 1986. Turbulent diffusion behind vehicles: experimentally determined turbulence mixing parameters. Atmos. Environ. 20, 851–860.
European Environment Agency (EEA), 2013. Environmental Topics. Urban Environment. http://www.eea.europa.eu/themes/urban.
Finnish Meteorological Institute, 2022a. The Emission Model Inventory for the Helsinki Metropolitan Area. FMI expert services – Air quality and energy (in Finnish). https://expo.fmi.fi/aqes/pub-lic/Paakaupunkiseudun_ilmanlaatuselvitys_2022.pdf.
Finnish Meteorological Institute, 2022b. The Emission Model Inventory for the Turku Region. FMI expert services – Air quality and energy (in Finnish). https://www.turku.fi/sites/default/files/atoms/files//turun_seudun_ilmanlaatuselvitys_2020.pdf.
Finnish Standards Association SFS, 1994. Air Protection. Bioindication. Moss Bag Method. Standard SFS 5794 (in Finnish). http://www.sfs.fi/en.
Fussel, J.C., Franklin, M., Green, D.C., Gustafsson, M., Harrison, R.M., Hicks, W., Kelly, F. J., Kishta, F., Miller, M.R., Mudway, I.S., Oroumiyeh, F., Selley, L., Wang, M., Zhu, Y., 2022. A review of road traffic-derived non-exhaus particles: emissions, physicochemical characteristics, health risks, and mitigation measures. Environ. Sci. Technol. 56, 6813–6835.
Gidhagen, L., Johansson, C., Langer, J., Olivares, G., 2004. Simulation of NOx and ultrafine particles in a street canyon in Stockholm, Sweden. Atmospheric International 38, 2029–2044.
Gómez, R.Q., Chaparro, M.A.E., Chaparro, M.A.E., Castañeda -Miranda, A.G., Marié, D. C., Garguilo, J.D., Böhnel, H.N., 2021. Magnetic biomonitoring using native Lichens: spatial distribution of traffic-derived particles. Water Air Soil Pollut. 232, 124.
Goryainova, Z., Vuković, G., Aničić Urošević, M., Vergel, K., Ostrovnya, T., Frontsayeva, M., Zechmeister, H., 2016. Assessment of vertical element distribution in street canyons using the moss *Sphagnum girgensohnii*: a case study in Belgrade and Moscow cities. Atmos. Pollut. Res. 7, 690–697.
Guyev, Y.A., Savory, E., 1999. Influence of street obstructions on flow processes within urban canyons. J. Wind Eng. Ind. Aerod. 82, 89–103.
Hellman, 2011. Liikenteen Sujuvuus Helsingissä 2011, Helsingin Kaupunkisuunnitteluviraston Julkaisuja 2011, vol. 3, p. 44. Liikenteen_sujuvuus_Helsingissä_2011_los_2011-3.pdf.
Hoydysh, W.G., Dabbert, W.F., 1998. Kinematics and dispersion characteristics of flows in asymmetric street canyons. Atmos. Environ. 22, 2677–2689.
Hu, W., Zhong, Q., 2010. Using the OSPM model on pollutant dispersion in an urban street canyon. Adv. Atmos. Sci. 27, 621–628.
Hueglin, C., Gehrig, R., Baltensperger, U., Gysel, Monn, C., Vonmont, H., 2005. Chemical characterisation of $PM_{2.5}$, PM_{10} and coarse particles at urban, near-city and rural sites. Atmos. Environ. 39, 637–651.
Hunt, A., Jones, J., Oldfield, F., 1984. Magnetic measurements and heavy metals in atmospheric particulates of anthropogenic origin. Sci. Total Environ. 33, 129–139.
Jackson, M., Worm, H.-U., Banerjee, S.K., 1990. Fourier analysis of digital hysteresis data: rock magnetic applications. Phys. Earth Planet. In. 65, 78–87.
Kauhaniemi, M., Kukkonen, J., Härkönen, J., Nikmo, J., Kangas, L., Omstedt, G., Ketzel, M., Kousa, A., Haakana, M., Karppinen, A., 2011. Evaluation of a road dust suspension model for predicting the concentrations of PM_{10} in a street canyon. Atmos. Environ. 45, 3646–3654.
Keskinen, J.-P., Auvinen, M., Hellsten, A., 2023. High-resolution Case Study of Pollutant Dispersion in an Urban Environment Using Large-Eddy Simulation. Air Pollution Modelling and its Application XXIX. In preparation.
Kim, J.J., Baik, J.J., 2001. Urban street canyon flows with bottom heating. Atmos. Environ. 35, 3395–3404.
Kumar, P., Fennell, P., Britter, R., 2008. Measurements of particles in the 5-1000 nm range close to road level in an urban street canyon. Sci. Total Environ. 390, 437–447.
Kumar, P., Fennell, P.S., Hayhurst, A.N., Britter, R.E., 2009a. Street versus rooftop level concentrations of fine particles in a Cambridge street canyon. Boundary-Layer Meteorol. 131, 3–18.
Kumar, P., Garmory, A., Ketzel, M., Berkowicz, R., Britter, R., 2009b. Comparative study of measured and modelled number concentrations of nanoparticles in an urban street canyon. Atmos. Environ. 43, 949–958.
Kumar, P., Ketzel, M., Vardoulakis, S., Pirjola, L., Britter, R., 2011. Dynamics and dispersion modelling of nanoparticles from road traffic in the urban atmospheric environment – a review. J. Aerosol Sci. 42, 580–603.
Kupiainen, K., 2007. Road dust from pavement wear and traction sanding. Monogr. Boreal Environ. Res. 26, 52. Finnish Environment Institute.
Lazić, L., Aničić Urošević, M., Mijić, Z., Vuković, G., Ilić, L., 2016. Traffic contribution to air pollution iin urban street canyons: integrated application of the OSPM, moss biomonitoring and spectral analysis. Atmos. Environ. 141, 347–360.
Limo, J., Paturi, P., Mäkinen, J., 2018. Magnetic biomonitoring with moss bags to assess stop-and-go traffic induced particulate matter and heavy metal concentration. Atmos. Environ. 195, 187–195.
Lu, S.-G., Bai, S.-Q., Cai, J.-B., Xu, C., 2005. Magnetic properties and heavy metal contents of automobile emission particulates. J. Zhejiang Univ. - Sci. 6B (8), 731–735.
Marié, D.C., Chaparro, M.A.E., Lavornia, J.M., Sinito, A.M., Castañeda-Miranda, A.G., Garguilo, J.D., Chaparro, M.A.E., Böhnel, H.N., 2018. Atmospheric pollution assessed in situ measurement of magnetic susceptibility of lichens. Ecol. Indicat. 95, 831–840.
Maronga, B., Gryschka, M., Heinze, R., Hoffmann, F., Kanani-Sühring, F., Keck, M., Ketelsen, K., Letzel, M.O., Sühring, M., Raasch, S., 2015. The Parallelized Large-Eddy Simulation Model (PALM) version 4.0 for atmospheric and oceanic flows: model formulation, recent developments, and future perspectives. Geosci. Model Dev. (GMD) 8, 2515–2551.
Maronga, B., Banzhaf, S., Burmeister, C., Esch, T., Forkel, R., Fröhlich, D., Fuka, V., Gehrke, K.F., Geletič, J., Giersch, S., Gronemeier, T., Groß, G., Heldens, W., Hellsten, A., Hoffmann, F., Inagaki, A., Kadasch, E., Kanani-Sühring, F., Ketelsen, K., Khan, B.A., Knigge, C., Koop, H., Krč, P., Kurppa, M., Maamari, H., Matzarakis, A., Mauder, M., Pallasch, M., Pavlik, D., Pfafferott, J., Resler, J., Rissmann, S., Russo, E., Salim, M., Schrempf, M., Schwenkel, J., Seckmeyer, G., Schubert, S., Sühring, M., von Tils, R., Vollmer, L., Ward, S., Witha, B., Wurps, H., Zeidler, J., Raasch, S., 2020. Overview of the PALM model system 6.0. Geosci. Model Dev. (GMD) 13, 1335–1372.
Mathias, A.D., Comrie, A.C., Musil, S.A., 2006. Atmospheric pollution. In: Pepper, I.L. (Ed.), Environmental and Pollution Science. Academic Press Inc., USA, pp. 377–394.
Matzka, J., Maher, B.A., 1999. Magnetic biomonitoring of roadside tree leaves: identification of spatial and temporal variations in vehicle-derived particulates. Atmos. Environ. 33 (Issue 28), 4565–4569.
Moreno, T., Pandolfi, M., Querol, X., Lavín, J., Alastuey, A., Viana, M., Gibbons, W., 2011. Manganese in the urban atmosphere: identifying anomalous concentrations and sources. Environ. Sci. Pollut. Control Ser. 18, 173–183.
Muxworthy, A.R., Lam, C., Green, D., Cowan, A., Maher, B.A., Gonet, T., 2022. Magnetic characterisation of London's airborne nanoparticulate matter. Atmos. Environ. 287, 119292.
Napier, F., D'Arcy, B., Jefferies, C., 2008. A review of vehicle related metals and polycyclic aromatic hydrocarbons in the UK environment. Desalination 226, 143150.
Omstedt, G., Bringfelt, B., Johansson, C., 2005. A model for vehicle-induced non-tailpipe emissions of particles along Swedish roads. Atmos. Environ. 39, 6088–6097.
Ottosen, T.-B., Kakosimos, K.E., Johansson, C., Hertel, O., Brandt, J., Skov, H., Berkowicz, R., Ellermann, T., Jensen, S.S., Ketzel, M., 2015. Analysis of the impact of inhomogeneous emissions in the operational street pollution model (OSPM). Geosci. Model Dev. (GMD) 8, 3231–3245.
Ozaki, H., Watanabe, I., Kuno, K., 2004. Investigation of the heavy metal sources in relation to automobiles. Water Air Soil Pollut. 157, 209–223.
Özkan, C., Bahtiyar, E., Deniz, A., 2016. Study on the association between air pollution and mortality in Istanbul, 2007-2012. Atmos. Pollut. Res. 7, 147–154.
Pakkanen, T.A., Kerminen, V.-M., Loukkola, K., Hillamo, R.E., Aarnio, P., Koskentalo, T., Maenhaut, W., 2003. Size distributions of mass and chemical components in street-level and rooftop PM_1 particles in Helsinki. Atmos. Environ. 37 (12), 1673–1690.
Park, S.-K., Kim, S.-D., Lee, H., 2004. Dispersion characteristics of vehicle emission in an urban street canyon. Sci. Total Environ. 323, 263–271.
Pirjola, L., Lähde, T., Niemi, J.V., Kousa, A., Rönkkö, T., Karjalainen, P., Keskinen, J., Frey, A., Hillamo, R., 2012. Spatial and temporal characterization of traffic emissions in urban microenvironments with a mobile laboratory. Atmos. Environ. 63, 156–167.
Pope, S.B., 2000. Turbulent Flows. Cambridge University Press.
Posada, D.B., Chaparro, M.A.E., Duque-Trujillo, J.F., 2023. Magnetic assessment of transplanted *Tillandsia* spp.: biomonitors of air particulate matter for high rainfall environments. Atmosphere 14, 213.
REDUST, 2014. Demonstration Test Final Report: Main Results and Conclusions, Deliverable Product of the REDUST LIFE Project Actions 1 and 2. http://www.ymk-projektit.fi/redust//files/2015/02/REDUST-Action-1-2-final-report.pdf.
Sagnotti, L., Macrì, P., Egli, R., Mondino, M., 2006. Magnetic properties of atmospheric particulate matter from automatic air sampler stations in Latium (Italy): toward a definition of magnetic fingerprints for natural and anthropogenic PM_{10} sources. J. Geophys. Res. 111, B12S22.

Salo, H., Mäkinen, J., 2019. Comparison of traditional moss bags and synthetic fabric bags in magnetic monitoring of urban air pollution. Ecol. Indicat. 104, 559–566.
Salo, H., Bućko, M., Vaahtovuo, E., Limo, J., Mäkinen, J., Pesonen, L., 2012. Biomonitoring of air pollution in SW Finland by magnetic and chemical measurements of moss bags and lichens. J. Geochem. Explor. 115, 69–81.
Sezgin, N., Ozcan, H.K., Deir, G., Nemlioglu, S., Bayat, C., 2003. Determination of heavy metal concentrations in street dusts in Istanbul E-5 highway. Environ. Int. 29, 979–985.
Sheikh, H.A., Maher, B.A., Karloukovski, V., Lampronti, G.I., Harrison, R.J., 2022. Biomagnetic characterization of air pollution particulates in Lahore, Pakistan. G-cubed 23 (2).
Shvetsova, M.S., Kamanina, I.Z., Frontasyeva, M.V., Madadzada, A.I., Zinicovscaia, I.I., Pavlov, S., Vergel, K.N., Yushin, N.S., 2019. Active moss biomonitoring using the "moss bag technique" in the park of moscow. Phys. Part. Nucl. Lett. 16 (6), 994–1003.
Sini, J.F., Anquentin, S., Mestayer, P.G., 1996. Pollutant dispersion and thermal effects in urban street canyons. Atmos. Environ. 30, 2659–2677.
Slezakova, K., Pereira, M.C., Reis, M.A., Alvim-Ferraz, M.C., 2007. Influence of traffic emissions on the composition of atmospheric particles of different sizes – Part 1: concentrations and elemental characterization. J. Atmos. Chem. 58, 55–68.
Solazzo, E., Vardoulakis, S., Cai, X., 2007. Evaluation of traffic-producing turbulence schemes within operating schemes within operational street pollution models using roadside measurements. Atmos. Environ. 41, 5357–5370.
Thorpe, A., Harrison, R.M., 2008. Sources and properties of non-exhaust particulate matter from road traffic: a review. Sci. Total Environ. 400, 270–282.
Tretiach, M., Pittao, E., Crisafulli, P., Adamo, P., 2011. Influence of exposure sites on trace element enrichment in moss-bags and characterization of particles deposited on the biomonitor surface. Sci. Total Environ. 409, 822–830.
Turku, 2016. Turun Kaupunkiseudun Ilmanlaatu Vuonna 2016, Turun Seudun Ilmansuojelun Yhteistyöryhmä. https://www.turku.fi/sites/default/files/atoms/files//ilmanlaatu_2016_yhdistetty.pdf.
Väkevä, M., Hämeri, K., Kulmala, M., Lahdes, R., Ruuskanen, J., Laitinen, T., 1999. Street level versus rooftop concentrations of submicron aerosol particles and gaseous pollutants in an urban street canyon. Atmos. Environ. 33 (9), 1385–1397.
van Laaten, N., von Tümpling, W., Merten, D., Bro, R., Schäfer, T., Pirrung, M., 2021. Spider web biomonitoring: a cost-effective source apportionment approach for urban particulate matter. Environ. Pollut. (Amsterdam, Neth.) 286, 117328.
Vardoulakis, S., Fisher, B.E.A., Pericleous, K., Gonzalez-Flesca, N., 2003. Modelling air quality in street canyons: a review. Atmos. Environ. 37, 155–182.
Vardoulakis, S., Valiantis, M., Milner, J., ApSimon, H., 2007. Operational air pollution modelling in the UK – street canyon applications and challenges. Atmos. Environ. 41, 4622–4637.
Viana, M., Querol, X., Alastuey, A., Gil, J.I., Menéndez, M., 2006. Identification of PM sources by principal component analysis (PCA) coupled with wind direction data. Chemosphere 65, 2411–2418.
Vuković, G., Aničić Urošević, M., Razumenić, I., Goryainova, Z., Frontasyeva, M., Tomašević, M., Popović, A., 2013. Active moss biomonitoring of small-scale spatial distribution of airborne major and trace elements in the Belgrade urban area. Environ. Sci. Pollut. Control Ser. 20, 5461–5470.
Vuković, G., Aničić Urošević, M., Tomašević, M., Samson, R., Popović, A., 2015. Biomagnetic monitoring of urban air pollution using moss bags (*Sphagnum girgensohnii*). Ecol. Indicat. 52, 40–47.
Wang, T., Xie, S., 2009. Assessment of traffic-related air pollution in the urban streets before and during the 20008 Beijing Olympic Games traffic control period. Atmos. Environ. 43, 5682–5690.
Ward, N.I., 1990. Multielement contamination of British motorway environments. Sci. Total Environ. 93, 393–401.
Weber, S., Kuttler, W., Weber, K., 2006. Flow charasteristics and particle mass and number concentration variability within a busy urban street canyon. Atmos. Environ. 40, 7565–7578.
Winkler, A., Carricchi, C., Guidotti, M., Owczarek, M., Macrì, P., Nazzari, M., Amoroso, A., Di Giosa, A., Listrani, S., 2019. Combined magnetic, chemical and morphoscopic analyses on lichens from a complex anthropic context in Rome, Italy. Sci. Total Environ. 690, 1355–1368.
Xie, X., Huang, Z., Wang, J., Xie, Z., 2005. Thermal effects on vehicle emission dispersion in an urban street canyon Transportation Research Part D. Transport and Environment 10, 197–212.
Yang, T., Liu, Q., Li, H., Zeng, Q., Chan, L., 2010. Anthropogenic magnetic particles and heavy metals in the road dust: magnetic identification and its implications. Atmos. Environ. 44, 1175–1185.
Zhang, K.M., Wexler, A.S., 2004. Evolution of particle number distribution near roadways-Part 1: analysis of aerosol dynamics and its implications for engine emission measurement. Atmos. Environ. 38, 6643–6653.
Zhu, Y., Hinds, W.C., Kim, S., Shen, S., Sioutas, C., 2002. Study of ultrafine particles near a major highway with heavy-duty diesel traffic. Atmos. Environ. 36, 4323–4335.
Zinicovscaia, I., Aničić Urošević, M., Vergel, K., Vieru, E., Frontasyeva, M.V., Povar, I., Duca, G., 2018. Active moss biomonitoring of trace elements air pollution in chisinau, Republic of Moldova. Ecological Cehimistry and Engineering 25 (3), 361–372. https://doi.org/10.1515/eces-2018-0024.